

Ozone and alkyl nitrate formation from the Deepwater Horizon oil spill atmospheric emissions

J. A. Neuman,^{1,2} K. C. Aikin,^{1,2} E. L. Atlas,³ D. R. Blake,⁴ J. S. Holloway,^{1,2} S. Meinardi,⁴ J. B. Nowak,^{1,2} D. D. Parrish,² J. Peischl,^{1,2} A. E. Perring,^{1,2} I. B. Pollack,^{1,2} J. M. Roberts,² T. B. Ryerson,² and M. Trainer²

Received 9 November 2011; revised 6 April 2012; accepted 9 April 2012; published 11 May 2012.

[1] Ozone (O_3), alkyl nitrates ($RONO_2$), and other photochemical products were formed in the atmosphere downwind from the Deepwater Horizon (DWH) oil spill by photochemical reactions of evaporating hydrocarbons with NO_x ($=NO + NO_2$) emissions from spill response activities. Reactive nitrogen species and volatile organic compounds (VOCs) were measured from an instrumented aircraft during daytime flights in the marine boundary layer downwind from the area of surfacing oil. A unique VOC mixture, where alkanes dominated the hydroxyl radical (OH) loss rate, was emitted into a clean marine environment, enabling a focused examination of O_3 and $RONO_2$ formation processes. In the atmospheric plume from DWH, the OH loss rate, an indicator of potential O_3 formation, was large and dominated by alkanes with between 5 and 10 carbons per molecule (C_5 – C_{10}). Observations showed that NO_x was oxidized very rapidly with a 0.8 h lifetime, producing primarily C_6 – C_{10} $RONO_2$ that accounted for 78% of the reactive nitrogen enhancements in the atmospheric plume 2.5 h downwind from DWH. Both observations and calculations of $RONO_2$ and O_3 production rates show that alkane oxidation dominated O_3 formation chemistry in the plume. Rapid and nearly complete oxidation of NO_x to $RONO_2$ effectively terminated O_3 production, with O_3 formation yields of 6.0 ± 0.5 ppbv O_3 per ppbv of NO_x oxidized. VOC mixing ratios were in large excess of NO_x , and additional NO_x would have formed additional O_3 in this plume. Analysis of measurements of VOCs, O_3 , and reactive nitrogen species and calculations of O_3 and $RONO_2$ production rates demonstrate that NO_x -VOC chemistry in the DWH plume is explained by known mechanisms.

Citation: Neuman, J. A., et al. (2012), Ozone and alkyl nitrate formation from the Deepwater Horizon oil spill atmospheric emissions, *J. Geophys. Res.*, 117, D09305, doi:10.1029/2011JD017150.

1. Introduction

[2] Tropospheric ozone (O_3) production caused by photochemical reactions between NO_x ($=NO + NO_2$) and volatile organic compounds (VOCs) has been studied extensively in urban, industrial, and rural environments [*National Research Council Committee on Tropospheric Ozone Formation and Measurement*, 1991]. VOCs react with the hydroxyl radical (OH) to produce peroxy radicals (RO_2 and HO_2) that rapidly

convert NO to NO_2 . Subsequent photolysis of NO_2 produces an oxygen atom that combines with molecular oxygen to form O_3 . Since NO_2 photolysis also produces NO, the process can cycle until NO_x is further oxidized, terminating the catalytic O_3 formation cycle.

[3] The initial VOC mixture and ratio to NO_x determines the effective catalytic chain length. Alkene oxidation can form relatively reactive secondary species such as aldehydes and peroxyacyl nitrates ($RC(O)O_2NO_2$) that propagate the O_3 formation cycle. In contrast, alkane oxidation forms less reactive secondary NO_x oxidation products and VOCs, primarily monofunctional alkyl nitrates ($RONO_2$) and ketones, which effectively terminate O_3 production [*Carter*, 1994]. Source characterization and photochemical processes in transported air masses have been analyzed by examining $RONO_2$ formation from anthropogenic emissions of alkane precursors [*Simpson et al.*, 2003; *Madronich*, 2006; *Simpson et al.*, 2006; *Reeves et al.*, 2007; *Worton et al.*, 2010]. Investigating these known processes in an environment with a unique VOC mixture provides a new opportunity to test our understanding of photochemical formation of O_3 and other secondary products.

¹Cooperative Institute for Research in Environmental Sciences, University of Colorado Boulder, Boulder, Colorado, USA.

²Chemical Sciences Division, Earth System Research Laboratory, NOAA, Boulder, Colorado, USA.

³Rosenstiel School of Marine and Atmospheric Science, University of Miami, Miami, Florida, USA.

⁴Department of Chemistry, University of California, Irvine, California, USA.

Corresponding author: A. Neuman, Cooperative Institute for Research in Environmental Sciences, University of Colorado Boulder, 325 Broadway, Boulder, CO 80305, USA. (andy.neuman@noaa.gov)

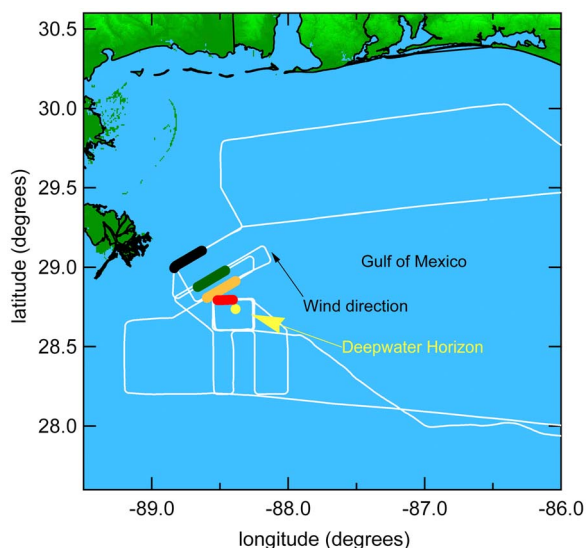


Figure 1. Map of the WP-3D flight track (white line) over the Gulf of Mexico on 10 June 2010. The yellow circle marks the location of the DWH oil platform. The aircraft sampled plumes in the atmospheric MBL at four distances downwind from DWH indicated by the thick bars: 10 km (red), 20 km (orange), 30 km (green), and 50 km (black).

[4] On 20 April 2010, an explosion and fire destroyed the Deepwater Horizon (DWH) offshore oil platform. For the ensuing three months, oil leaked from the wellhead at the seafloor, 1520 m below the surface in the Gulf of Mexico. Large amounts of oil from the DWH spill reached the ocean surface and promptly evaporated [Ryerson *et al.*, 2011]. Measurements in and over the ocean showed that little methane [Yvon-Lewis *et al.*, 2011] and other light alkanes [Ryerson *et al.*, 2011] were released to the atmosphere, since they nearly fully dissolved in the seawater. The unique speciation of the VOC mixture released to the atmosphere from this deep-water oil spill provided a new environment for examination of tropospheric photochemistry [e.g., de Gouw *et al.*, 2011], particularly that initiated by OH oxidation of relatively heavy alkanes. Such a large emission of VOCs into a remote marine environment enabled a study of secondary photochemical products without the confounding influences of a multitude of sources [Neuman *et al.*, 2009] and broad mix of VOCs typically found over the continent. Spill response efforts emitted NO_x from ship exhaust, surface oil burning, and flaring of recovered gas into the atmosphere in the vicinity of the oil spill. The subsequent gas-phase photochemical reactions between NO_x and hydrocarbons evaporating from the surface oil slick are studied in the downwind plume from DWH. In particular, O₃ and the RONO₂ oxidation products formed from reactions between these NO_x and VOC emissions are examined in detail.

2. Measurements

[5] The National Oceanic and Atmospheric Administration (NOAA) WP-3D instrumented aircraft flew over the Gulf of Mexico in the vicinity of DWH on 8 and 10 June 2010. The aircraft sampled the plume of DWH emissions during the daytime at altitudes between 60 and 200 m above

the sea surface and well within the well-mixed marine boundary layer (MBL) that was approximately 600 m deep [Ryerson *et al.*, 2011]. Figure 1 shows a map of the region and the flight track of the aircraft on 10 June 2010. The gas-phase species studied here were emitted from a small area and remained confined to a narrow plume, spreading less than 10 km horizontally at 50 km downwind. On 10 June, the winds in the MBL were steady out of the southeast at 5.7 ± 0.4 m/s [Ryerson *et al.*, 2011, auxiliary material] at the locations and times that the WP-3D sampled the DWH plume. The colored portions of the flight track in Figure 1 indicate four locations at 10, 20, 30, and 50 km downwind from DWH where the plume was repeatedly sampled to capture chemical transformations during transport. Atmospheric transport times calculated from the average wind speed and the distance from DWH to the plume sampling locations were approximately 0.5, 1.0, 1.5, and 2.5 h in the four transects shown in Figure 1.

[6] This analysis uses fast-response in situ measurements of reactive nitrogen species, O₃, and meteorological parameters, and measurements of VOCs and RONO₂ in whole air canister samples. All data are publicly available at <http://esrl.noaa.gov/csd/tropchem/2010gulf/>. Independent chemical ionization mass spectrometer instruments measured nitric acid (HNO₃) [Neuman *et al.*, 2002] and peroxyacetyl nitrate (PAN; CH₃C(O)O₂NO₂), [Shusher *et al.*, 2004] with uncertainties of $\pm(15\% + 0.040$ ppbv) and $\pm(20\% + 0.005$ ppbv), respectively. NO, NO₂, NO_y (=NO + NO₂ + PAN + HNO₃ + RONO₂ + ...) and O₃ measured by chemiluminescence were reported once per second with uncertainties of $\pm(3\% + 0.01$ ppbv), $\pm(4\% + 0.03$ ppbv), $\pm(12\% + 0.10)$ ppbv, and $\pm(2\% + 0.015$ ppbv), respectively [Ryerson *et al.*, 1998, 1999; Pollack *et al.*, 2011]. Carbon monoxide (CO) was measured with 5% uncertainty by vacuum ultraviolet fluorescence [Holloway *et al.*, 2000], and methane (CH₄) was measured by cavity ringdown spectroscopy [Chen *et al.*, 2010]. Speciated VOCs and RONO₂ were determined by gas chromatography with flame ionization or mass spectrometric analysis of 72 whole air samples collected in stainless steel canisters on each flight [Colman *et al.*, 2001]. Each canister was filled in approximately 4 s and the sampling was manually initiated to target the plume from DWH. Eight RONO₂ compounds with between one and five carbon atoms per molecule were measured with $\pm 10\%$ accuracy, and in a few samples the sum of C₆–C₈ RONO₂ were estimated with approximately $\pm 50\%$ uncertainty (D. R. Blake, personal communication, 2011). The estimates of the C₆–C₈ RONO₂ mixing ratios were made by assuming all chromatogram peaks that appeared at retention times larger than the pentyl nitrates were heavier alkyl nitrates, and that the detector response for the heavier alkyl nitrates was the same as for the lighter nitrates. Since longer chain (>C₈) RONO₂ were likely lost in the analytical system, C₉–C₁₁ RONO₂ were not measured here. VOCs measured in the canisters include aromatics, alkenes, and 27 linear and branched alkanes with up to 11 carbons per molecule (C₁₁) [Ryerson *et al.*, 2011]. Accuracies for the VOCs analyzed here were typically $\pm 10\%$.

3. Results

[7] Only the 10 June results are analyzed in detail below, since transport times could not be determined unambiguously

Table 1. Trace Gas Mixing Ratios Measured on 10 June 2010 in the MBL Below 0.2 km Altitude Over the Gulf of Mexico in Two Plumes From DWH and Upwind of DWH^a

Species	10 km Downwind (ppbv)	50 km Downwind (ppbv)	Upwind (ppbv)
NO _y	9.3	2.7	0.6
NO ₂	4.8	0.12	0.01
CO	139	140	133
methane/1000	1888	1887	1882
ethane	1.4	1.2	1.1
propane	2.7	0.8	0.164
n-butane	21.7	4.9	0.020
n-pentane	29.8	7.4	0.009
n-hexane	25.1	6.7	0.008
methylcyclohexane	25.4	6.6	0.009
n-octane	15.3	4.2	0.011
n-nonane	13.2	3.9	0.012
n-decane	8.8	3.0	0.012
m+p xylene	7.3	1.2	<0.003
1,2,4 trimethylbenzene	3.5	0.6	<0.003

^aTwo plumes from DWH are shown in Figure 4. Only the most abundant alkane and aromatic isomers are listed.

under the light and variable winds that prevailed during the 8 June flight. However, the enhancement ratios of trace gases were similar on the 8 June and 10 June flights, suggesting that the findings are representative of photochemical processing in the DWH plume.

3.1. Atmospheric VOC Abundance

[8] Downwind from DWH, the mixture of atmospheric VOCs from evaporating surface oil was markedly different from VOC mixtures in other urban, industrial, and remote environments that have been investigated. Upwind from DWH, background concentrations of C₅–C₁₀ alkanes in the Gulf of Mexico MBL were less than 20 pptv (Table 1), consistent with measurements from a research vessel in 2006 in the same region [Gilman *et al.*, 2009]. In the DWH plumes measured here, many C₅–C₁₀ alkanes exceeded 10 ppbv (Table 1), and were considerably more abundant than generally found in U.S. urban and industrial areas [Baker *et al.*, 2008; Jobson *et al.*, 2004]. Furthermore, the mass flux of the measured VOCs in the DWH plumes was independent (within approximately 50% uncertainties) of downwind distance [Ryerson *et al.*, 2011, Figure 3a], indicating negligible VOC loss within the transport times examined here. In highly concentrated urban and petrochemical industrial plumes sampled near Houston, Texas, peak C₅–C₁₀ alkane mixing ratios were similar to the levels measured here [Gilman *et al.*, 2009; Ryerson *et al.*, 2003; Washenfelder *et al.*, 2010]; however, C₂–C₄ alkanes and alkenes were even more abundant than the C₅–C₁₀ alkanes in the Houston plumes. VOC speciation in the DWH plume was characterized by extremely high concentrations of C₅–C₁₀ alkanes without corresponding enhancements in lighter alkanes or alkenes. Heavier aromatics also were present in the atmospheric DWH plumes at ppbv-levels (Table 1), whereas lighter aromatics such as benzene and toluene were not substantially enhanced because they were efficiently dissolved in the ocean [Ryerson *et al.*, 2011].

3.2. Contributions to OH Loss Rate

[9] Measurements of VOCs and other trace gases downwind of DWH are used to calculate OH loss rates, which are the product of a compound's concentration with its rate coefficient for reaction with OH (k_{OH}). O₃ formation is favored when VOCs that propagate photochemical reactions dominate the OH loss rate, while O₃ formation is inhibited when compounds that form unreactive secondary products dominate the OH loss rate. For example, a large OH loss rate from NO₂ suppresses O₃ formation, because NO₂ reacts with OH to form HNO₃. Since HNO₃ formation removes NO_x and OH radicals from rapid photochemical reactions [Neuman *et al.*, 2006], it can represent a terminating step in O₃ formation photochemistry.

[10] The OH loss rate of compounds measured in the DWH plume over the Gulf of Mexico was dominated by C₅–C₁₀ alkanes and C₈–C₉ aromatics. Figure 2 compares OH loss rates for alkanes and aromatics measured in a plume 10 km downwind from DWH to similar measurements in freshly emitted urban and petrochemical plumes. The great abundance of these alkanes in all plume transects (ranging from 0.5 to 2.5 h downwind) caused the OH loss rate from the sum of the measured C₅–C₁₀ alkanes to exceed 10 s⁻¹ in all DWH plume transects, with the greatest contributions from several C₇ alkanes. The OH loss rate from aromatics was dominated by C₉ molecules and was less than a fourth the loss rate from alkanes. Alkane mixing ratios greatly exceeded alkene mixing ratios, such that the OH loss rate from total alkenes was negligible even though alkenes have larger k_{OH} . In contrast, in plumes influenced by Houston petrochemical emissions, alkenes with large k_{OH} dominated the OH loss rate (Figure 2), even though they were not the most abundant VOCs [Ryerson *et al.*, 2003; Washenfelder *et al.*, 2010]. NO₂ levels in the DWH plume (Table 1) were much less than found in many urban locations, where the OH loss rate can be dominated by NO₂ (e.g., the Dallas plume, Figure 2). The OH loss rate from NO₂ was less than 1 s⁻¹ even in the closest DWH plume transects with the highest NO₂ concentrations. CO and CH₄ in the DWH plume were not substantially enhanced above background, and OH loss rates from these compounds were less than 1 s⁻¹, similar to that in the upwind marine atmosphere. In summary, the emission plume from DWH represents a unique chemical regime where high OH loss rates were dominated by C₅–C₁₀ alkanes, while NO₂, CO, CH₄, and alkenes made relatively small contributions to the OH loss rate. The effects on NO_x oxidation and O₃ formation rates and yields are examined below.

3.3. NO_x Oxidation Rate

[11] In the MBL near DWH, NO_x emissions from ships, flaring of recovered gas, and other response operations mixed with VOCs evaporating from the surfaced oil. On 10 June, peak NO_x mixing ratios of 10 ppbv from these recovery operations were 2–3 orders of magnitude greater than the 20–50 pptv background NO_x outside the plume (Table 1).

[12] NO_y is a measurement of NO_x and its oxidation products [Fahey *et al.*, 1986]. NO_y is a conserved tracer of NO_x emissions, assuming negligible loss of reactive nitrogen species, which is a good approximation on these short

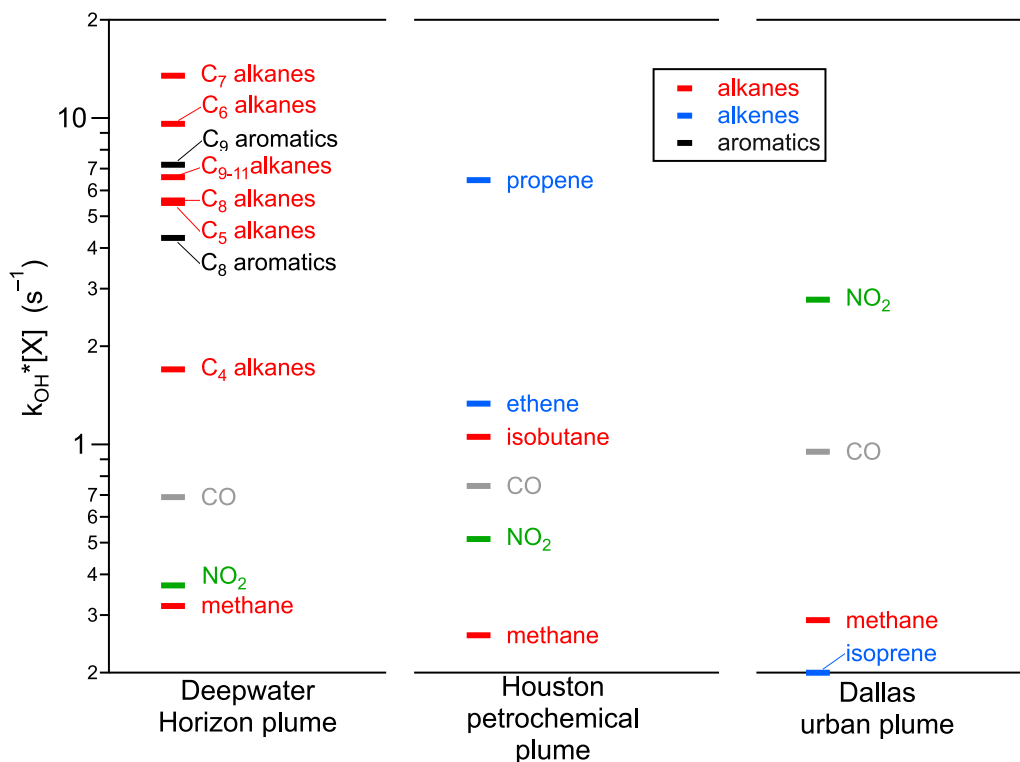


Figure 2. OH loss rates greater than 0.2 s^{-1} in a plume 10 km downwind from DWH plume on 10 June 2010 (shown in Figure 4a and Table 1), compared to OH loss rates in a plume downwind from Houston petrochemical industrial emissions [Ryerson *et al.*, 2003] and over the Dallas urban area on 25 September 2006. The individually measured compounds that contributed to the carbon number groupings in the DWH plume are: C₄ alkanes = isobutane + n-butane, C₅ alkanes = isopentane + n-pentane + cyclopentane, C₆ alkanes = n-hexane + cyclohexane + 2-methylpentane + 3-methylpentane + methylcyclopentane, C₇ alkanes = n-heptane + 2-methylhexane + 3-methylhexane + methylcyclohexane, C₈ alkanes = n-octane + 2-methylheptane, C₉₋₁₁ alkanes = n-nonane + n-decane + undecane, C₈ aromatics = ethylbenzene + m, o, and p-xylenes, C₉ aromatics = 1,2,3-trimethylbenzene + 1,3,5-trimethylbenzene + 1,2,4-trimethylbenzene + n-propylbenzene + 3-ethyltoluene + 4-ethyltoluene.

time scales (≤ 2.5 h). Reactive nitrogen is emitted from combustion sources primarily as NO, and the ratio of plume NO_x to NO_y (NO_x:NO_y) approaches unity at the time of emission. NO_x:NO_y decreases over time as NO_x is oxidized to other NO_y species during transport downwind, and the change in the ratio quantifies NO_x oxidation in the plume. NO_x and NO_y were highly correlated in the DWH plume transects, with $r^2 > 0.97$ in all but the most aged plumes, where $r^2 = 0.84$. NO_x:NO_y, determined from linear least squares fits to the data from each crosswind plume transect, versus plume transport time is shown in Figure 3a. Ten km downwind from DWH, NO_x:NO_y was 0.817 ± 0.005 ppbv/ppbv, indicating that almost 20% of the emitted NO_x already had been oxidized in these plumes that had aged only 0.5 h since emission. NO_x:NO_y decreased rapidly with further plume transport, reaching 0.06 at 2.5 h and 50 km downwind. The NO_x photochemical lifetime, determined from a linear least squares fit of the logarithm of NO_x:NO_y measured in each plume transect versus transport time, was unusually short at 0.83 ± 0.16 h (solid line in Figure 3a). NO_x loss by OH + NO₂ was negligible here, as demonstrated by the absence of HNO₃ production in the plumes (Figure 4). Instead, the rapid NO_x loss was caused by the reaction of peroxy radicals with NO (discussed in section 3.5

below). In comparison, NO_x lifetimes in power plant plumes were 6 h [Ryerson *et al.*, 1998], and those in VOC-rich plumes from Houston petrochemical industrial sources were 1.8 h (dashed line, Figure 3a) [Ryerson *et al.*, 2003]. The extremely rapid decrease of NO_x:NO_y downwind from DWH shows that the chemistry was prompt with essentially complete NO_x oxidation within three hours.

3.4. NO_x Oxidation Products

[13] The secondary oxidation products from NO_x-VOC photochemistry reveal the atmospheric processes responsible for the rapid NO_x oxidation. Figure 4 illustrates temporal changes in reactive nitrogen partitioning in the DWH plume. In fresh plumes (e.g., Figure 4a), NO_x accounted for over 80% of plume NO_y. In aged plumes (e.g., Figure 4b), NO_x oxidation was nearly complete, but NO_x, PAN, HNO₃, and the sum of eight C₁-C₅ RONO₂ accounted for only 22% of plume NO_y. This result differs dramatically from previous studies, where the sum of NO_x + PAN + HNO₃ accounted for over 96% of NO_y in urban and petrochemical plumes [Neuman *et al.*, 2002; Ryerson *et al.*, 2003] and for approximately 90% of NO_y in rural areas [Parrish *et al.*, 1993]. In urban air masses, RONO₂ often accounted for a few percent of NO_y [O'Brien *et al.*, 1997; Flocke *et al.*,

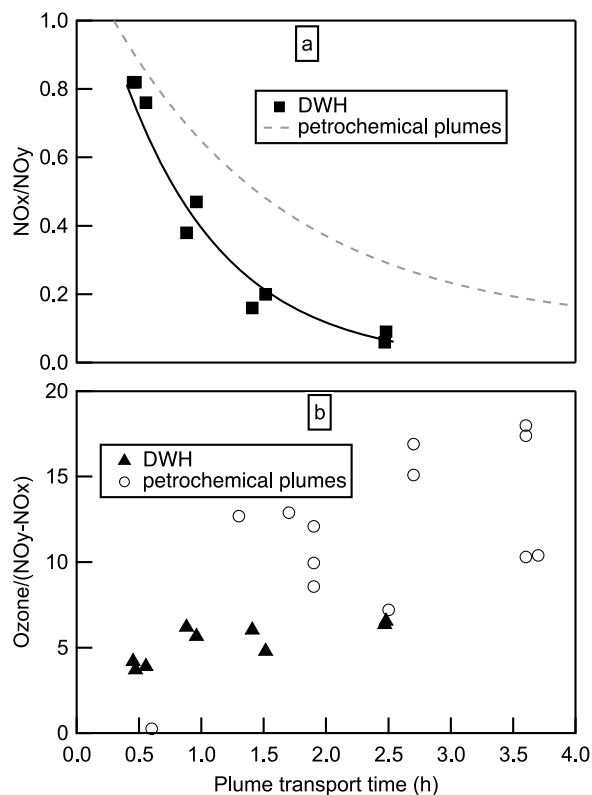


Figure 3. (a) NO_x to NO_y enhancement ratios measured in nine DWH plume transects versus downwind transport time. The solid line is a fit to the data. (b) The ozone production efficiency (OPE) determined from the ratio of O₃ to NO_y–NO_x measured in the same plume transects are shown as closed triangles. For comparison, NO_x lifetimes (dashed line in Figure 3a) and OPE in Houston petrochemical industrial plumes (open circles in Figure 3b) from *Ryerson et al.* [2003] are shown.

1998; *Schneider et al.*, 1998; *Talbot et al.*, 2003; *Ryerson et al.*, 2003], and up to 10–20% of NO_y in some studies [*Day et al.*, 2003; *Perring et al.*, 2010].

[14] The NO_x oxidation products that account for the majority of NO_y in the aged plumes were not measured directly here, but they can be inferred from the measurements. Although heavier RONO₂ were not reported regularly from the whole air samples, C₆–C₈ RONO₂ were measured with approximately 50% uncertainty in selected canisters in DWH plumes [described in section 2 above]. For example, near the center of the plume 50 km and 2.5 h downwind from DWH (Figure 4b), most NO_x was oxidized and PAN and HNO₃ formation was small. Where the canister was sampled closest to the plume center, the difference between NO_y and (NO_x + PAN + HNO₃) was approximately 1 ppbv. The C₁–C₅ RONO₂ were enhanced by 60 pptv, and the C₆–C₈ RONO₂ were enhanced by several hundred pptv (not shown). Although >C₈ RONO₂ were not measured here, their mixing ratios are expected to be substantially increased since their production rate from the measured parent alkanes is calculated to be large [section 3.5]. The large difference between NO_y and the sum of the individually measured compounds was only apparent in aged DWH plumes. Although all alkyl nitrates are not measured here, the

observations are consistent with RONO₂ species with more than 5 carbon atoms accounting for the majority of reactive nitrogen in aged DWH plumes.

3.5. Alkyl Nitrate Production Estimated From VOC Measurements

[15] The presence of long chain RONO₂ in aged DWH plumes suggested by the NO_y difference measurements is supported by calculations of RONO₂ abundance and speciation in the DWH plume using measurements of the parent

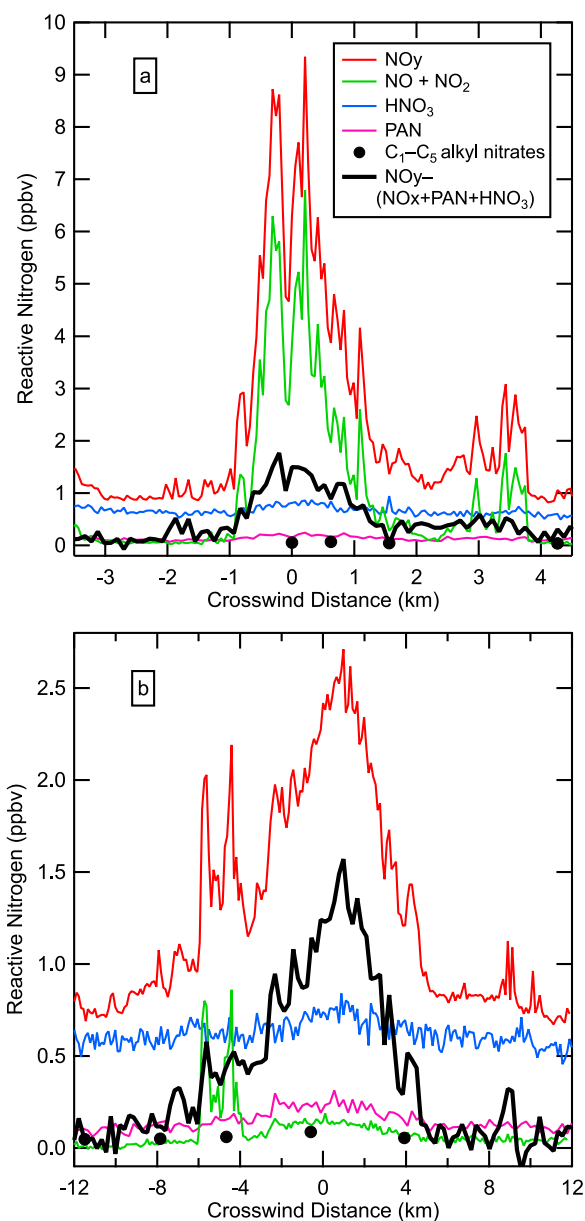


Figure 4. Time series of reactive nitrogen species measured on 10 June 2010 in the MBL in plumes (a) 10 km and (b) 50 km downwind from DWH. NO_x, NO_y, and HNO₃ were measured once per s and PAN was measured once per 2 s. C₁–C₅ alkyl nitrates were measured in whole air samples at locations indicated by the circles. The sum of alkyl nitrates (black lines) is inferred from the difference between NO_y and (NO_x + PAN + HNO₃).

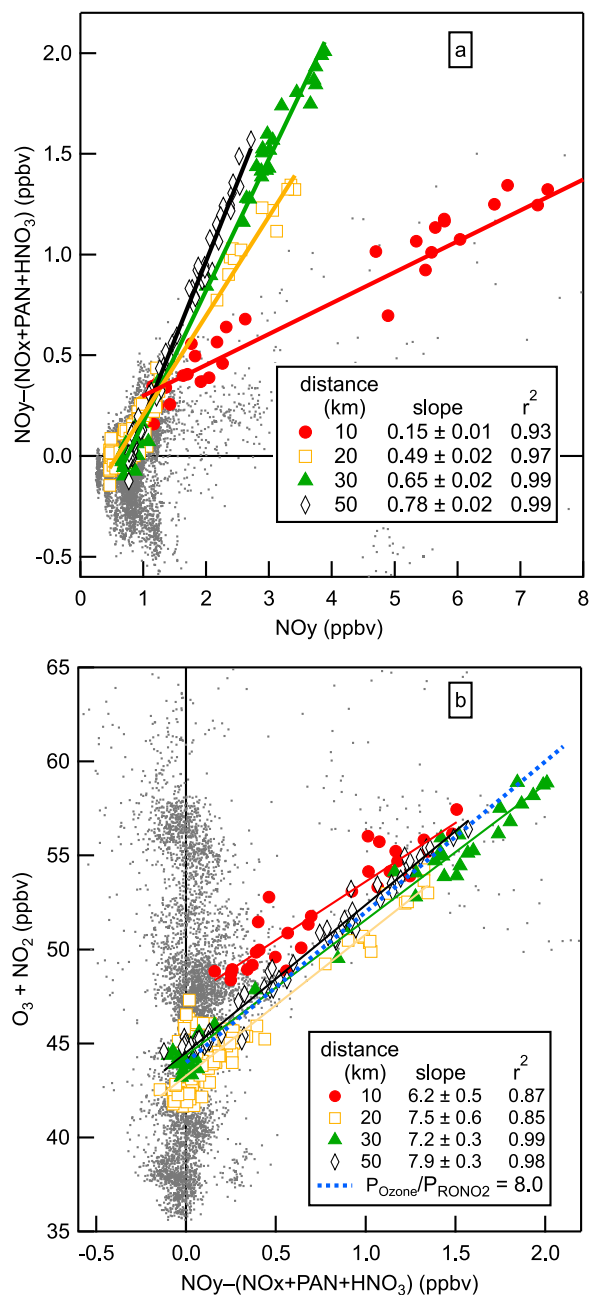


Figure 5. The 1-s measurements of (a) $\text{NO}_y - (\text{NO}_x + \text{PAN} + \text{HNO}_3)$ versus NO_y (gray dots) and (b) $\text{O}_3 + \text{NO}_2$ versus $\text{NO}_y - (\text{NO}_x + \text{PAN} + \text{HNO}_3)$ (gray dots) over the Gulf of Mexico on the 10 June 2010 WP-3D flight. Colored symbols indicate measurements in four plume transects 10 km (red), 20 km (orange), 30 km (green), and 50 km (black) downwind from DWH. Lines through the colored points are the linear least squares fits to the data from a single plume transect. The correlation slope for each line is shown with 95% confidence intervals. The blue dashed line in Figure 5b is the calculated ratio of O_3 to RONO_2 production rates from section 3.6.

alkanes. The RONO_2 production rate (P_{RONO_2}) from each parent VOC is determined from the measured VOC concentration, k_{OH} for that VOC, and the branching ratio for RONO_2 formation (β) from the reaction of the product RO_2 with NO [Atkinson *et al.*, 1982; Roberts, 1990; Arey *et al.*, 2001; Perring *et al.*, 2010] as

$$P_{\text{RONO}_2} = \beta \times k_{\text{OH}} \times [\text{OH}][\text{VOC}]. \quad (1)$$

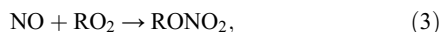
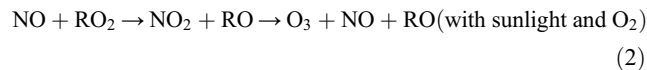
Summation of equation (1) over all VOCs gives the total RONO_2 production rate. The largest contribution to the total calculated RONO_2 production rate is from $\text{C}_6\text{--C}_{10}$ alkanes, which were responsible for 80% of the RONO_2 production. In the aged DWH plumes, the RONO_2 production rate was dominated by oxidation of these long chain alkanes because their mixing ratios (Table 1), RONO_2 branching ratios, and k_{OH} [Atkinson *et al.*, 1982; Roberts, 1990] were large. The ratio of calculated RONO_2 production rates for the sum of $\text{C}_1\text{--C}_{11}$ RONO_2 (ΣRONO_2) compared to the sum of $\text{C}_1\text{--C}_5$ RONO_2 is 20. Hence, the measured 60 pptv enhancement in the sum of $\text{C}_1\text{--C}_5$ RONO_2 in the aged DWH plume (Figure 4b) suggests a greater than 1 ppbv enhancement in ΣRONO_2 . The ΣRONO_2 calculated from measurements of the parent VOC mixing ratios is consistent with $\text{NO}_y - (\text{NO}_x + \text{PAN} + \text{HNO}_3)$ measured in the aged DWH plume shown in Figure 4b, demonstrating that $\text{NO}_y - (\text{NO}_x + \text{PAN} + \text{HNO}_3)$ accurately represents ΣRONO_2 .

[16] The difference between NO_y and $(\text{NO}_x + \text{PAN} + \text{HNO}_3)$ increased as the DWH plume aged during downwind transport. Figure 5 shows 1 s measurements of $\text{NO}_y - (\text{NO}_x + \text{PAN} + \text{HNO}_3)$ versus NO_y in the MBL over the Gulf of Mexico on 10 June. Many of the gray points with minimal $\text{NO}_y - (\text{NO}_x + \text{PAN} + \text{HNO}_3)$ and increased O_3 were obtained in the northern portion of the flight shown in Figure 1, where air masses with continental origins were sampled. These measurements outside the DWH plume demonstrate that $\text{NO}_x + \text{PAN} + \text{HNO}_3$ usually accounted for the majority of NO_y , and that O_3 was not ordinarily correlated with $\text{NO}_y - (\text{NO}_x + \text{PAN} + \text{HNO}_3)$. Similarly, only small differences between NO_y and $(\text{NO}_x + \text{PAN} + \text{HNO}_3)$ have been reported in other environments, demonstrating that $(\text{NO}_x + \text{PAN} + \text{HNO}_3)$ accounted for most of NO_y elsewhere (discussed in section 3.4). The slopes of linear least squares fits to the plume data have high correlation coefficients, with r^2 ranging from 0.93 to 0.99. The ΣRONO_2 fraction of plume NO_y is inferred from $\text{NO}_y - (\text{NO}_x + \text{PAN} + \text{HNO}_3)$ versus NO_y correlation slopes. $\Sigma\text{RONO}_2/\text{NO}_y$ enhancement ratios measured in plume transects increased monotonically with distance from 10 to 50 km downwind from DWH, rising from 0.15 (red line in Figure 5a) to 0.78 (black line in Figure 5a). Substantial RONO_2 production in the DWH plume confirms that oxidation of heavier alkanes dominated the $\text{NO}_x\text{--VOC}$ chemistry.

3.6. Photochemical Ozone Production

[17] The elevated alkane concentrations in the DWH plumes led to rapid O_3 formation, but radical termination by RONO_2 formation limited the O_3 yield. Comparing calculated to observed O_3 production rates in the DWH plume identifies the processes responsible for O_3 formation. Although O_3 and RONO_2 production rate calculation

requires knowledge of OH, which was not measured from the aircraft, the ratio of O₃ to RONO₂ production is independent of OH. Reactions of RO₂ with NO produce both O₃ (reaction 2) and RONO₂ (reaction 3) [Roberts, 1990];



where R is an alkyl group and RO is an alkoxy radical. Thus, RONO₂ and O₃ production rates are related by the branching between RONO₂ formation (which terminates O₃ production) and NO₂ formation (which leads to O₃ production and NO regeneration, thus continuing O₃ production). Since reaction of RO₂ with NO is rapid compared to RO₂ formation from reaction of OH with VOCs, the RONO₂ production rate from an individual VOC is given by equation (1), and the O₃ production rate (P_{O₃}) is given by

$$P_{\text{O}_3} = \gamma \times (1 - \beta) \times k_{\text{OH}} \times [\text{OH}][\text{VOC}], \quad (4)$$

where γ is the number of O₃ molecules formed from reaction 2. Since reaction 2 usually leads to one O₃ from NO₂ photolysis and another from subsequent reactions of RO, γ is approximately 2. Total O₃ and RONO₂ production rates from a VOC mixture are obtained by summing the production rates given by equations (1) and (4) for each VOC. Using equations (1) and (4) with k_{OH} and β from Perring *et al.* [2010], the ratio P_{O₃}/P_{RONO₂} is calculated from measured parent VOC concentrations. Assuming that VOC measurement inaccuracy of $\pm 10\%$ dominates the uncertainties in equations (1) and (4), then summing the two equations over the average VOC speciation in the DWH plume [Ryerson *et al.*, 2011] gives P_{O₃}/P_{RONO₂} = 8.0 \pm 0.8.

[18] P_{O₃}/P_{RONO₂} also can be determined from O₃ and RONO₂ measurements in the DWH plume and compared to the above value to test if the calculations accurately represent the chemistry. Since O₃ and RONO₂ have a common source and negligible depositional or photochemical losses [Talukdar *et al.*, 1997] on the short time scales here, the observed O₃ to Σ RONO₂ enhancement ratio in the DWH plume is equivalent to the ratio of their production rates. Figure 5b shows 1-s measurements of O₃ (represented by O₃ + NO₂ to account for titration of O₃ by NO) versus Σ RONO₂ (inferred from the difference between measured NO_y and (NO_x + PAN + HNO₃)). Over the Gulf of Mexico and outside the DWH plume (gray dots in Figure 5b), Σ RONO₂ determined from NO_y - (NO_x + PAN + HNO₃) averaged -0.02 ± 0.18 ppbv and was uncorrelated with O₃. Four DWH plume transects are colored as in Figures 1 and 5a. P_{O₃}/P_{RONO₂} is inferred from the correlation slope of linear least squares fits of O₃ to Σ RONO₂ observed in each plume transect. O₃ and Σ RONO₂ were enhanced and highly correlated in the DWH plume transects, with r^2 values ranging from 0.87 to 0.99. In the earliest plume transect 0.5 h downwind, the O₃ to RONO₂ correlation slope was 6.2 ± 0.5 (red line in Figure 5b), and the slope rapidly increased to 7.5 ± 0.4 in transects 20–50 km downwind. Within the measurement uncertainties, this observed ratio of production rates agrees with the calculated P_{O₃}/P_{RONO₂} (blue

dashed line in Figure 5b) demonstrating that OH oxidation of the measured VOCs accurately describes the O₃ photochemistry and RONO₂ production in the DWH plume.

4. Discussion and Conclusions

[19] The release of gas and oil from the deep ocean resulted in a unique atmospheric VOC mixture that allowed O₃ photochemistry from alkanes to be studied in isolation from reactions of other VOCs. The effective branching ratio for production of RONO₂ depends on the VOC composition and characterizes the NO_x-VOC chemistry that produces O₃. Effective branching ratio determinations are valuable for predicting changes in O₃ formation in response to VOC reductions [Farmer *et al.*, 2011]. By combining equations (1) and (4) and considering all VOCs,

$$P_{\text{O}_3}/P_{\text{RONO}_2} = \gamma(1 - \beta_e)/\beta_e, \quad (5)$$

where β_e is the effective branching ratio of the entire VOC mixture. Both observed O₃ to Σ RONO₂ ratios and production rate calculations using measured VOCs determine $\beta_e = 0.2$ in the DWH plume. β_e was considerably higher here than in urban and rural environments, where effective branching ratios ranged from 0.03 to 0.10 [Farmer *et al.*, 2011; Perring *et al.*, 2010]. RONO₂ branching ratios increase with n-alkane carbon number [Atkinson *et al.*, 1982; Roberts, 1990], and large straight-chain alkanes have branching ratios as high as 0.47 for n-decane. In the DWH plume, C₅–C₁₀ alkanes dominated the VOC mixture making β_e uncommonly large. The relatively large β_e in the DWH plume shifted the NO_x-VOC chemistry toward RONO₂ production, at the expense of O₃ formation.

[20] Ozone production efficiency (OPE), which can be determined observationally from the ratio of O₃ to NO_x oxidation products, is used regularly as a metric to assess O₃ photochemistry [e.g., Trainer *et al.*, 1993; Neuman *et al.*, 2009]. The difference NO_y–NO_x represents the sum of all NO_x oxidation products. Since NO_y was effectively conserved on the short time scales studied here (≤ 2.5 h), we interpret the correlation slope from linear least squares fits of measured O₃ to NO_y–NO_x as net OPE. In the DWH plume, OPE was 6.0 ± 0.5 ppbv/ppbv after 1 h of transport (Figure 3b), and similar to values measured in U.S. urban areas [Trainer *et al.*, 1995; Neuman *et al.*, 2009]. In contrast, petrochemical plumes with OH loss rates dominated by alkenes had OPEs ranging from 10 to 18 [Ryerson *et al.*, 2003] (Figure 3b). On 10 June, O₃ enhancements in the DWH plumes were less than 15 ppbv (Figure 5b), even after NO_x was completely oxidized. Although the ratio of VOC to NO_x was very large, O₃ production was limited by OH oxidation of C₅–C₁₀ alkanes that preferentially formed RONO₂ and by NO_x levels less than 10 ppbv.

[21] Reactive nitrogen partitioning indicates that O₃ production had effectively ceased in the plumes observed 50 km downwind. NO_x had been nearly completely oxidized, and there was little PAN formation that could catalyze later O₃ production. NO_x oxidation in the atmospheric DWH plume favored RONO₂ production, and approximately 1 h after emission, reactive nitrogen was dominated by RONO₂. Since the RONO₂ species have photochemical lifetimes of many days [Talukdar *et al.*, 1997] and do not readily

decompose to release NO_x, their formation represents a terminating step in NO_x-VOC photochemistry on short time scales. The nearly constant relationship between O₃ and RONO₂ (inferred from the difference between NO_y and individually measured compounds) in plumes aged between 1 and 2.5 h (Figure 5b) confirms that net O₃ production terminated once RONO₂ were formed and that RONO₂ were not removed rapidly from the atmosphere. The fate of these RONO₂ in the atmosphere is slow decomposition by reaction with OH or photolysis over many days or weeks [Roberts, 1990; Kames and Schurath, 1992; Clemitshaw et al., 1997; Talukdar et al., 1997].

[22] VOCs were considerably more abundant than NO_x in the DWH plume and were still substantially enhanced after NO_x was depleted. For example, during the 0.5 h transport time between transects 10 and 20 km downwind, n-heptane remained nearly constant and over 15 ppbv, whereas NO_x decreased from 7 to 2 ppbv. Although O₃ formation had ceased after NO_x was oxidized, efficient plume transport of VOCs from DWH to regions with additional NO_x emissions (over land, for example) may initiate further O₃ formation. The measurements and calculations presented here reveal the gas-phase photochemical processes and the resulting secondary reaction products in the DWH plume, and demonstrate that NO_x-VOC chemistry in this unique atmospheric VOC mixture is explained by known mechanisms.

[23] **Acknowledgments.** We thank the NOAA Climate Change, Health of the Atmosphere Program for support and the NOAA Aircraft Operation Center staff for accomplishing the Gulf flights.

References

- Arey, J., S. M. Aschmann, E. S. C. Kwok, and R. Atkinson (2001), Alkyl nitrate, hydroxyalkyl nitrate, and hydroxycarbonyl formation from the NO_x-air photooxidations of C₅-C₈ n-alkanes, *J. Phys. Chem. A*, *105*, 1020–1027, doi:10.1021/jp003292z.
- Atkinson, R., S. M. Aschmann, W. P. L. Carter, A. M. Winer, and J. N. Pitts Jr. (1982), Alkyl nitrate formation from the NO_x-air photooxidations of C₂-C₈ n-alkanes, *J. Phys. Chem.*, *86*, 4563–4569, doi:10.1021/j100220a022.
- Baker, A. K., A. J. Beyersdorf, L. A. Doezem, A. Katzenstein, S. Meinardi, I. J. Simpson, D. R. Blake, and F. S. Rowland (2008), Measurements of nonmethane hydrocarbons in 28 United States cities, *Atmos. Environ.*, *42*, 170–182, doi:10.1016/j.atmosenv.2007.09.007.
- Carter, W. P. L. (1994), Development of ozone reactivity scales for volatile organic compounds, *J. Air Waste Manage. Assoc.*, *44*, 881–899.
- Chen, H., et al. (2010), High-accuracy continuous airborne measurements of greenhouse gases (CO₂ and CH₄) using the cavity ring-down spectroscopy (CRDS) technique, *Atmos. Meas. Tech.*, *3*(2), 375–386, doi:10.5194/amt-3-375-2010.
- Clemitshaw, K. C., J. Williams, O. V. Rattigan, D. E. Shallcross, K. S. Law, and R. A. Cox (1997), Gas-phase ultraviolet absorption cross-sections and atmospheric lifetimes of several C₂-C₅ alkyl nitrates, *J. Photochem. Photobiol. A*, *102*, 117–126, doi:10.1016/S1010-6030(96)04458-9.
- Colman, J. J., A. L. Swanson, S. Meinardi, B. Sive, D. R. Blake, and F. S. Rowland (2001), Description of the analysis of a wide range of volatile organic compounds in whole air samples collected during PEM-Tropics A and B, *Anal. Chem.*, *73*, 3723–3731, doi:10.1021/ac010027g.
- Day, D. A., M. B. Dillon, P. J. Wooldridge, J. A. Thornton, R. S. Rosen, E. C. Wood, and R. C. Cohen (2003), On alkyl nitrates, O₃, and the “missing NO_y,” *J. Geophys. Res.*, *108*(D16), 4501, doi:10.1029/2003JD003685.
- de Gouw, J. A., et al. (2011), Organic aerosol formation downwind from the Deepwater Horizon oil spill, *Science*, *331*, 1295–1299, doi:10.1126/science.1200320.
- Fahey, D. W., G. Hubler, D. D. Parrish, E. J. Williams, R. B. Norton, B. A. Ridley, H. B. Singh, S. C. Liu, and F. C. Fehsenfeld (1986), Reactive nitrogen species in the troposphere: Measurements of NO, NO₂, HNO₃, particulate nitrate, peroxyacetyl nitrate (PAN), O₃, and total reactive odd nitrogen (NO_y) at Niwot Ridge, Colorado, *J. Geophys. Res.*, *91*(D9), 9781–9793, doi:10.1029/JD091iD09p09781.
- Farmer, D. K., et al. (2011), Impact of organic nitrates on urban ozone production, *Atmos. Chem. Phys.*, *11*, 4085–4094, doi:10.5194/acp-11-4085-2011.
- Flocke, F., A. Volz-Thomas, H.-J. Buers, W. Pätz, H.-J. Garthe, and D. Kley (1998), Long-term measurements of alkyl nitrates in southern Germany: 1. General behavior and seasonal and diurnal variation, *J. Geophys. Res.*, *103*, 5729–5746, doi:10.1029/97JD03461.
- Gilman, J. B., et al. (2009), Measurements of volatile organic compounds during the 2006 TexAQSGoMACCS campaign: Industrial influences, regional characteristics, and diurnal dependencies of the OH reactivity, *J. Geophys. Res.*, *114*, D00F06, doi:10.1029/2008JD011525.
- Holloway, J. S., R. O. Jakoubek, D. D. Parrish, C. Gerbig, A. Volz-Thomas, S. Schmitgen, A. Fried, B. Wert, B. Henry, and J. R. Drummond (2000), Airborne intercomparison of vacuum ultraviolet fluorescence and tunable diode laser absorption measurements of tropospheric carbon monoxide, *J. Geophys. Res.*, *105*, 24,251–24,261, doi:10.1029/2000JD900237.
- Jobson, B. T., C. M. Berkowitz, W. C. Kuster, P. D. Goldan, E. J. Williams, F. C. Fehsenfeld, E. C. Apel, T. Karl, W. A. Lonneman, and D. Riemer (2004), Hydrocarbon source signatures in Houston, Texas: Influence of the petrochemical industry, *J. Geophys. Res.*, *109*, D24305, doi:10.1029/2004JD004887.
- Kames, J., and U. Schurath (1992), Alkyl nitrates and bifunctional nitrates of atmospheric interest: Henry's Law constants and their temperature dependencies, *J. Atmos. Chem.*, *15*, 79–95, doi:10.1007/BF00053611.
- Madronich, S. (2006), Chemical evolution of gaseous air pollutants downwind of tropical megacities: Mexico City case study, *Atmos. Environ.*, *40*, 6012–6018, doi:10.1016/j.atmosenv.2005.08.047.
- National Research Council Committee on Tropospheric Ozone Formation and Measurement (1991), *Rethinking the Ozone Problem in Urban and Regional Air Pollution*, Natl. Acad. Press, Washington, D. C.
- Neuman, J. A., et al. (2002), Fast-response airborne in situ measurements of HNO₃ during the Texas 2000 Air Quality Study, *J. Geophys. Res.*, *107*(D20), 4436, doi:10.1029/2001JD001437.
- Neuman, J. A., et al. (2006), Reactive nitrogen transport and photochemistry in urban plumes over the North Atlantic Ocean, *J. Geophys. Res.*, *111*, D23S54, doi:10.1029/2005JD007010.
- Neuman, J. A., et al. (2009), Relationship between photochemical ozone production and NO_x oxidation in Houston, Texas, *J. Geophys. Res.*, *114*, D00F08, doi:10.1029/2008JD011688.
- O'Brien, J. M., P. B. Shepson, Q. Wu, T. Biesenthal, J. W. Bottenheim, H. A. Wiebe, K. G. Anlauf, and P. Brickell (1997), Production and distribution of organic nitrates, and their relationship to carbonyl compounds in an urban environment, *Atmos. Environ.*, *31*(14), 2059–2069, doi:10.1016/S1352-2310(97)80002-7.
- Parrish, D. D., et al. (1993), The total reactive oxidized nitrogen levels and the partitioning between the individual species at six rural sites in eastern North America, *J. Geophys. Res.*, *98*(D2), 2927–2939, doi:10.1029/92JD02384.
- Perring, A. E., et al. (2010), The production and persistence of ΣRONO₂ in the Mexico City plume, *Atmos. Chem. Phys.*, *10*, 7215–7229, doi:10.5194/acp-10-7215-2010.
- Pollack, I. B., B. M. Lerner, and T. B. Ryerson (2011), Evaluation of ultraviolet light-emitting diodes for detection of atmospheric NO₂ by photolysis - chemiluminescence, *J. Atmos. Chem.*, *65*(2), 111–125, doi:10.1007/s10874-011-9184-3.
- Reeves, C. E., et al. (2007), Alkyl nitrates in outflow from North America over the North Atlantic during Intercontinental Transport of Ozone and Precursors 2004, *J. Geophys. Res.*, *112*, D10S37, doi:10.1029/2006JD007567.
- Roberts, J. M. (1990), The atmospheric chemistry of organic nitrates, *Atmos. Environ., Part A*, *24*, 243–287.
- Ryerson, T. B., et al. (1998), Emission lifetimes and ozone formation in power plant plumes, *J. Geophys. Res.*, *103*, 22,569–22,583, doi:10.1029/98JD01620.
- Ryerson, T. B., L. G. Huey, K. Knapp, J. A. Neuman, D. D. Parrish, D. T. Sueper, and F. C. Fehsenfeld (1999), Design and initial characterization of an inlet for gas-phase NO_y measurements from aircraft, *J. Geophys. Res.*, *104*, 5483–5492, doi:10.1029/1998JD100087.
- Ryerson, T. B., et al. (2003), Effect of petrochemical industrial emissions of reactive alkenes and NO_x on tropospheric ozone formation in Houston, Texas, *J. Geophys. Res.*, *108*(D8), 4249, doi:10.1029/2002JD003070.
- Ryerson, T. B., et al. (2011), Atmospheric emissions from the Deepwater Horizon spill constrain air-water partitioning, hydrocarbon fate, and leak rate, *Geophys. Res. Lett.*, *38*, L07803, doi:10.1029/2011GL046726.
- Schneider, M., O. Luxenhofer, A. Deissler, and K. Ballschmiter (1998), C₁-C₁₅ alkyl nitrates, benzyl nitrate, and bifunctional nitrates: Measurements in California and South Atlantic air and global comparison using C₂Cl₄ and CHBr₃ as marker molecules, *Environ. Sci. Technol.*, *32*(20), 3055–3062, doi:10.1021/es980132g.

- Simpson, I. J., N. J. Blake, D. R. Blake, E. Atlas, F. Flocke, J. H. Crawford, H. E. Fuelberg, C. M. Kiley, S. Meinardi, and F. S. Rowland (2003), Photochemical production and evolution of selected C₂–C₅ alkyl nitrates in tropospheric air influenced by Asian outflow, *J. Geophys. Res.*, *108*(D20), 8808, doi:10.1029/2002JD002830.
- Simpson, I. J., T. Wang, H. Guo, Y. H. Kwok, F. Flocke, E. Atlas, S. Meinardi, F. S. Rowland, and D. R. Blake (2006), Long-term atmospheric measurements of C₁–C₅ alkyl nitrates in the Pearl River Delta region of southeast China, *Atmos. Environ.*, *40*, 1619–1632, doi:10.1016/j.atmosenv.2005.10.062.
- Slusher, D. L., L. G. Huey, D. J. Tanner, F. M. Flocke, and J. M. Roberts (2004), A thermal dissociation-chemical ionization mass spectrometry (TD-CIMS) technique for the simultaneous measurement of peroxyacyl nitrates and dinitrogen pentoxide, *J. Geophys. Res.*, *109*, D19315, doi:10.1029/2004JD004670.
- Talbot, R., et al. (2003), Reactive nitrogen in Asian continental outflow over the western Pacific: Results from the NASA Transport and Chemical Evolution over the Pacific (TRACE-P) airborne mission, *J. Geophys. Res.*, *108*(D20), 8803, doi:10.1029/2002JD003129.
- Talukdar, R. K., J. B. Burkholder, M. Hunter, M. K. Gilles, J. M. Roberts, and A. R. Ravishankara (1997), Atmospheric fate of several alkyl nitrates, *J. Chem. Soc. Faraday Trans.*, *93*(16), 2797–2805, doi:10.1039/a701781b.
- Trainer, M., et al. (1993), Correlation of ozone with NO_y in photochemically aged air, *J. Geophys. Res.*, *98*, 2917–2925, doi:10.1029/92JD01910.
- Trainer, M., B. A. Ridley, M. P. Buhr, G. Kok, J. Walega, G. Hübler, D. D. Parrish, and F. C. Fehsenfeld (1995), Regional ozone and urban plumes in the southeastern United States: Birmingham, a case study, *J. Geophys. Res.*, *100*, 18,823–18,834, doi:10.1029/95JD01641.
- Washenfelder, R. A., et al. (2010), Characterization of NO_x, SO₂, ethene, and propene from industrial emission sources in Houston, Texas, *J. Geophys. Res.*, *115*, D16311, doi:10.1029/2009JD013645.
- Worton, D. R., et al. (2010), Alkyl nitrate photochemistry during the tropospheric organic chemistry experiment, *Atmos. Environ.*, *44*, 773–785, doi:10.1016/j.atmosenv.2009.11.038.
- Yvon-Lewis, S. A., L. Hu, and J. Kessler (2011), Methane flux to the atmosphere from the Deepwater Horizon oil disaster, *Geophys. Res. Lett.*, *38*, L01602, doi:10.1029/2010GL045928.